DOI: 10.1002/zaac.201300279

Zinc(II) and Nickel(II) Complexes Based on Schiff Base Ligands: Synthesis, Crystal Structure, Luminescent and Magnetic Properties

Xiaoting Qin,[a] Yufei Ji,[a] Yanfei Gao,[a] Lei Yan,[a] Shuai Ding,[a] Yanqin Wang,[a] and Zhiliang Liu*[a,b]

Keywords: Schiff base ligands; Zinc; Nickel; Luminescence; Magnetic properties

Abstract. Three new phenolate oxygen bridged transition metal complexes $[Zn_3(HL^1)_3(\mu_3\text{-}CH_3O)]\cdot(ClO_4)_2(H_2O)_3$ (**1**), $[Ni_2(HL^1)_2(\mu_{1,1}\text{-}N_3)$(o-vanillin)$]\cdot H_2O$ (**2**), $[Ni_3(HL^2)_2(PhCOO)_2(PhCOOH)_2(EtOH)_2]$ (**3**) have been synthesized by metal ions and potentially multidentate Schiff base ligands (H_2L^1 = 2-((1-hydroxy-2-methylpropan-2-ylimino) methyl)-6-methoxyphenol; H_3L^2 = (*E*)-1-((2-hydroxy-3-methoxybenzylidene)amino)ethane-1,2-diol). All the three complexes **1**, **2**, and **3** have been characterized by elemental analysis, FT-IR spectroscopy, and single-crystal X-ray diffraction studies. Crystal structures reveal that complex **1** is a trinuclear incomplete cubane-like zinc cluster whereas complex **2** is a dinuclear nickel complex bridged by azide, and compound **3** is a trinuclear nickel complex. The luminescent property for complex **1** and magnetic behaviors for complexes **2** and **3** have been investigated.

Introduction

Transition-metal complexes are of unabated interest because of their fascinating structural topologies, such as poly-nuclear clusters,[1] one-dimensional chains,[2] two-dimensional layers,[3] and three-dimensional frameworks especially MOFs (metal-organic frameworks),[4] and potential applications in a wide range of areas as functional materials including magnetism,[5] luminescence,[6] catalysis,[7] sensors,[8] nonlinear optics,[9] and ion exchange.[10] In general, the structural motifs and properties of these hybrid compounds are closely related to the metal centers and the coordinated multidentate ligands. Schiff bases are a preferred ligand class for cluster synthesis, since a) they are polydentate ligands with diverse N and O donor sites, b) they exhibit various coordination modes, and c) the multiple coordination/ ligation modes of these ligands easily lead to the synthesis of coordination complexes. For the metal centers, much attention has been focused on the zinc(II) and nickel(II) complexes. A number of studies concentrate on zinc(II) Schiff base complexes in terms of luminescence[11] and catalysis.[12] The design and synthesis of nickel(II) compounds based on Schiff base chelates arouses continuous interests for their interesting magnetic properties.[13]

In this work, *o*-vanillin reacts with amino alcohol 2-amino-2-methyl-1-propanol and 3-amino-1,2-propanediol to obtain the Schiff base ligands H_2L^1[14] and H_3L^2, respectively (see Scheme 1). The Schiff base H_2L^1 is a tetradentate ligand featuring NO_3 (one nitrogen atom and three oxygen atoms) donor sites whereas H_3L^2 is a new pentadentate Schiff base ligand accompanying NO_4 (one nitrogen atom and four oxygen atoms) donor sites. Our intention is the use of these two Schiff base ligands with zinc and nickel ions to construct numbers of new polynuclear complexes with aesthetically pleasing structures and fascinating properties. Finally, three new complexes were synthesized and structurally characterized by single-crystal X-ray diffraction.

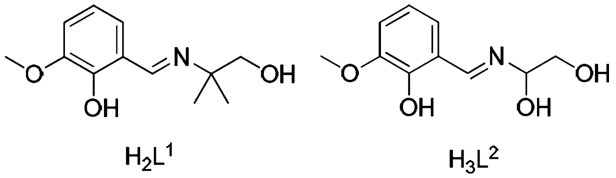

Scheme 1. Structure of Schiff base ligands in this paper.

Results and Discussion

Description of Crystal Structures

Structure of $[Zn_3(HL^1)_3(\mu_3\text{-}CH_3O)]\cdot(ClO_4)_2(H_2O)_3$ (1)

X-ray crystallographic analysis shows that complex **1** crystallizes in the triclinic space group $P\bar{1}$. The structure of **1** consists of a $[Zn_3(HL^1)_3(\mu_3\text{-}CH_3O)]^{2+}$ cation, two isolated perchlorate anions and three solvent water molecules. Selected bond lengths and angles for complex **1** are presented in Table 1. As shown in Figure 1, the trinuclear zinc(II) core of complex **1** consists of three metal ions, one deprotonated methanol group and three Schiff base ligands $(HL^1)^-$, which acts in a tetradentate mode. The coordination environments of the

---

* Prof. Dr. Z. Liu
Fax: +86-471-4992147
E-Mail: cezlliu@imu.edu.cn
[a] College of Chemistry and Chemical Engineering
Inner Mongolia University
Hohhot, 010021, P. R. China
[b] Key Lab of Nanoscience and Nanotechnology
Inner Mongolia
Hohhot, 010021, P. R. China

Table 1. Selected bond lengths /Å and bond angles /° for complex **1**.

bond lengths /Å							
Zn1–N1	2.028(5)	Zn1–O6	1.979(4)	Zn2–O6	2.012(4)	Zn3–O3	1.970(5)
Zn1–O1	2.130(4)	Zn2–N2	2.026(5)	Zn2–O9	1.989(4)	Zn3–O8	2.124(6)
Zn1–O2	2.142(5)	Zn2–O1	2.101(4)	Zn3–N3	2.026(5)	Zn3–O9	1.999(4)
Zn1–O3	2.013(4)	Zn2–O5	2.101(6)	Zn3–O1	2.097(4)		
bond angles /°							
N1–Zn1–O1	131.60(18)	O6–Zn1–O3	102.45(19)	O9–Zn2–O1	81.03(17)	O3–Zn3–N3	142.90(19)
N1–Zn1–O2	79.8(2)	N2–Zn2–O1	136.7(2)	O9–Zn2–O5	97.3(2)	O3–Zn3–O1	81.32(17)
O1–Zn1–O2	93.37(19)	N2–Zn2–O5	78.9(2)	O9–Zn2–O6	104.6(2)	O3–Zn3–O8	96.6(2)
O3–Zn1–N1	89.53(19)	O5–Zn2–O1	95.5(2)	N3–Zn3–O1	135.31(19)	O3–Zn3–O9	104.4(2)
O3–Zn1–O1	79.54(18)	O6–Zn2–N2	88.7(2)	N3–Zn3–O8	78.5(2)	O9–Zn3–N3	90.0(2)
O6–Zn1–O1	79.99(17)	O6–Zn2–O1	79.97(17)	O1–Zn3–O8	93.3(2)	O9–Zn3–O1	80.88(17)
O6–Zn1–O2	96.4(2)	O9–Zn2–N2	142.2(2)				

three metal atoms are similar; each of them is hexacoordinated exhibiting considerably distorted octahedral geometry. The six coordination sites of Zn1 are occupied by phenolate oxygen O3 and O6, hydroxyl oxygen O2, alkoxyl O7, imino N1 from two different Schiff base ligands and oxygen atom O1 of the μ_3-methanol oxygen atom. Three central metal ions interconnect through two types of oxygen bridges afforded by the μ_2-phenolate oxygen from Schiff base ligand and the μ_3-oxygen from deprotonated methanol group, respectively, constituting an incomplete cubane-like $[Zn_3O_4]^{2+}$ core with the Zn–O bond lengths in the range of 1.963(6)–2.137(7) Å. In the incomplete cubane-like $[Zn_3O_4]^{2+}$ core, the Zn–O–Zn' angles are in the range of 94.962(2)–103.665(3)° and the O–Zn–O' angles are in the range of 79.403(2)–81.230(2)°, which are in accordance with those in previously reported cubane-like complexes.[15]

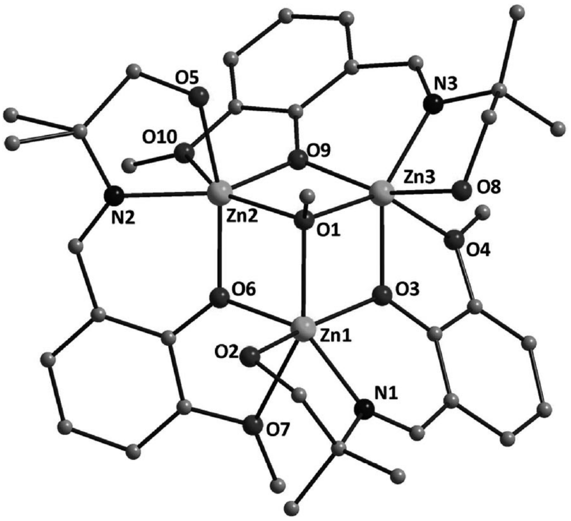

Figure 1. Coordination environment for complex **1**, the hydrogen atoms, solvent molecules and perchlorate counterion are omitted for clarity.

Structure of $[Ni_2(HL^1)_2(\mu_{1,1}\text{-}N_3)(o\text{-vanillin})]\cdot H_2O$ (2)

X-ray crystallographic analysis shows that complex **2** crystallizes in the triclinic space group $P\bar{1}$. A perspective view of the molecule structure with atom numbering is depicted in Figure 2. Selected bond lengths and angles for complex **2** are presented in Table 2. The structure of **2** consists of a neutral, well-separated binuclear unit $[Ni_2(HL^1)_2(\mu_{1,1}\text{-}N_3)(o\text{-vanillin})]$ and one crystallographic water molecule. The metal atoms of the dinuclear compound are linked by one nitrogen atom N3 from the azide group in end-on (EO) fashion and one phenolate oxygen atom O1 from *o*-vanillin in a tridentate manner. Each nickel ion is coordinated to one Schiff base ligand $(HL^1)^-$, which acts in a tridentate mode, with one hydroxy oxygen atom, one deprotonated phenolate oxygen atom and one imino nitrogen atom coordinated. The Ni^{II} ions are hexacoordinated exhibiting slightly distorted octahedral coordination environment. The equatorial plane for Ni1 consists of the imino N1, phenolate oxygen O1, alkoxyl O3 and N3 from azide group. The axial positions of Ni1 are occupied by phenolate oxygen O5 and hydroxyl oxygen O4 both from Schiff base ligand. The Ni2 ion shows similar coordination geometry except that aldehyde oxygen instead of alkoxyl in the axial. The Ni–O distances are in the range of 1.978(2)–2.300(3) Å and Ni–N distances are in the range of 1.993(3)–2.150(2) Å. The Ni···Ni distance between two central metal ions is 3.1822(7) Å. All these distances are very close to those of the previously reported Ni_2 complexes.[16] Furthermore, intra- and inter- molecular hydrogen bonding interactions existing in the complex as

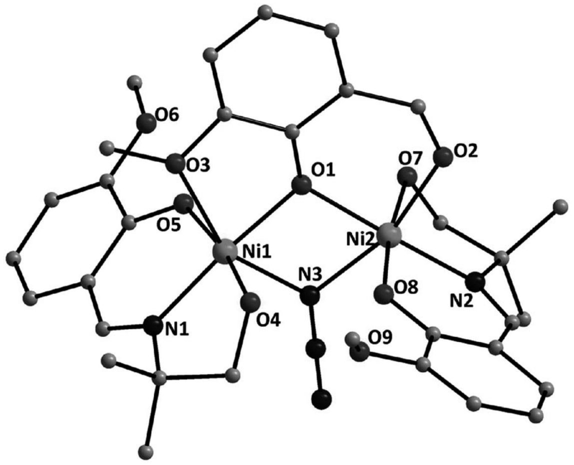

Figure 2. Coordination environment for complex **2**, the hydrogen atoms and solvent molecule are omitted for clarity.

Table 2. Selected bond lengths /Å and bond angles /° for complex **2**.

bond lengths /Å							
Ni1–O1	2.008(2)	Ni1–O4	2.101(2)	Ni2–O1	2.005(2)	Ni2–O7	2.093(2)
Ni1–O5	1.978(2)	Ni1–N3	2.101(3)	Ni2–O8	1.970(2)	Ni2–N3	2.150(2)
Ni1–N1	1.993(3)	Ni1–O3	2.300(3)	Ni2–N2	1.996(3)	Ni2–O2	2.087(2)
bond angles /°							
O1–Ni1–O4	86.78(9)	O5–Ni1–O3	84.43(10)	O1–Ni2–O7	94.22(9)	O8–Ni2–O2	93.10(10)
O1–Ni1–N3	77.80(9)	N1–Ni1–O4	80.32(10)	O1–Ni2–N3	76.72(9)	N2–Ni2–O7	80.86(10)
O1–Ni1–O3	73.67(9)	N1–Ni1–N3	104.60(10)	O1–Ni2–O2	87.52(9)	N2–Ni2–N3	101.87(10)
O5–Ni1–O1	99.84(9)	N1–Ni1–O3	103.94(10)	O8–Ni2–O1	92.57(9)	N2–Ni2–O2	93.52(10)
O5–Ni1–N1	92.63(10)	O4–Ni1–O3	89.48(10)	O8–Ni2–N2	92.39(10)	O7–Ni2–N3	92.24(10)
O5–Ni1–N3	97.37(10)	N3–Ni1–O4	92.18(10)	O8–Ni2–N3	91.03(10)	O2–Ni2–O7	85.44(10)

listed in Table 3. As shown in Figure 3, hydroxyl group –O4H4 is hydrogen bonded to the alkoxyl oxygen atom O9 and the phenolate oxygen atom O8. Two hydrogen atoms H10D, H10E of the lattice water molecular are engaged in two hydrogen bonding, respectively. And the oxygen atom O10 of the lattice water molecular is hydrogen bonded to the hydroxyl group –O7H7 to result in an H-bonded dimeric entity.

Table 3. Hydrogen bond lengths /Å and bond angles /° for complex **2**.

D–H···A	d(D–H)	d(H···A)	d(D···A)	DHA
O7–H7···O10^1	0.840(10)	2.107(13)	2.888(5)	155(2)
O4–H4···O8	0.849(10)	1.775(18)	2.593(3)	161(4)
O4–H4···O9	0.849(10)	2.56(4)	3.118(4)	125(3)
O10–H10D···O1^2	0.844(10)	2.59(5)	3.128(4)	123(5)
O10–H10D···O7^2	0.844(10)	1.88(3)	2.664(4)	154(6)
O10–H10E···O5^2	0.846(10)	2.10(5)	2.756(3)	133(6)
O10–H10E···O6^2	0.846(10)	2.50(6)	2.960(4)	115(5)

Symmetry transformations used to generate equivalent atoms: ^{1} 1–*x*, 2–*y*, –*z*; ^{2} –1+*x*, +*y*, +*z*.

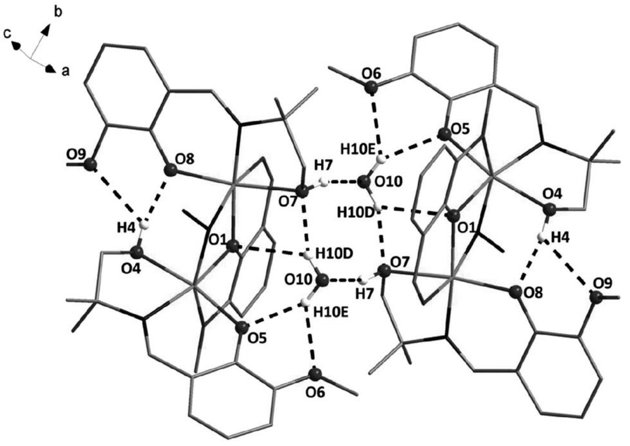

Figure 3. Hydrogen bonding interactions of complex **2**.

Structure of [Ni$_3$(HL^2)$_2$(PhCOO)$_2$(PhCOOH)$_2$(EtOH)$_2$] (3)

X-ray crystallographic analysis shows that complex **3** crystallizes in the monoclinic space group *C*2/*c*. Half of the neutral compound **3** is contained in the asymmetric unit, with the other half generated by a twofold axis. Selected bond lengths and angles for complex **3** are presented in Table 4. As shown in Figure 4, this compound contains three hexacoordinate nickel ions which are bonded to two Schiff base ligands, two ethanol molecules and four benzoates with two different types of coordination of carboxylic groups. The Schiff base ligand acts in a tetradentate mode. The metal atoms Ni1 and Ni2 are connected through one deprotonated μ$_2$-phenolate oxygen atom of ligand (HL^2)$^{2–}$ and one μ$_2$-carboxyl group of benzoate ion. Finally, there are two monocoordinated PhCOOH molecules to complete the coordination sphere of Ni2 and Ni2A. The central metal Ni1 atom is bonded to six oxygen atoms in a slightly distorted octahedral coordination environment with the Ni1–O distances in a range of 2.023(3)–2.088(3) Å, and the O–Ni1–O' angles in a range of 78.15(12)–102.51(12)°. The other two metallic atoms Ni2 and Ni2A are surrounded by five oxygen atoms and one nitrogen atom with slightly distorted octahedral arrangement. The Ni2–O distances are in the range of 2.029(3)–2.129(3) Å and Ni2–N distance is 2.014(4) Å. The Ni···Ni distance between two adjacent nickel atoms is 3.4841(12) Å, the Ni2···Ni1···Ni2A angle is 146.247(14)°. All of them are within the normal range as reported in other literature.[17]

Luminescent Properties

The fluorescence properties of the Schiff base ligand H$_2$L^1 and its Zn^{II} complex **1** were investigated at room temperature (298 K) in the solid state (see Figure 5). Upon the irradiation of ultraviolet light, the emission maximum wavelength for complex **1** is 483 nm upon excitation 395nm, and the emission maximum wavelength for the H$_2$L^1 ligand is 540 nm upon excitation 468 nm. The emission spectrum shows that the Zn^{II} complex **1** displays much stronger emission intensity than that of Schiff base ligand H$_2$L^1 with a slightly blue-shift. The weaker fluorescence of the ligand is related to the occurrence of a photoinduced electron transfer (PET) process due to the presence of a lone pair of electrons of the donor atoms in the ligand (N, O-donor).[18] Complex **1** exhibits stronger emission fluorescence tentatively attributable to the PET process is prevented by the complexation of ligand with metal ions. Furthermore, the fluorescence intensity may be greatly enhanced by the ligation between the ligand and the stable d^{10} zinc metal centers which effectively increases the rigidity of the ligand and reduces the loss of energy by nonradioactive decay.[19]

Table 4. Selected bond lengths /Å and bond angles /° for complex **3**.

bond lengths /Å							
Ni1–O1	2.024(3)	Ni2–O2	2.028(3)	Ni2–O5	2.122(3)	Ni2–O8	2.129(3)
Ni1–O6	2.033(3)	Ni2–O3	2.053(4)	Ni2–O6	2.029(3)	Ni2–N1	2.009(4)
Ni1–O7	2.086(3)						
bond angles /°							
O1–Ni1–O1^1	88.86(17)	O6–Ni1–O7^1	93.71(11)	N1–Ni2–O8	90.91(17)	O3–Ni2–O5	90.47(13)
O1^1–Ni1–O6^1	102.36(11)	O7^1–Ni1–O7	88.56(19)	O2–Ni2–O3	89.79(13)	O5–Ni2–O8	91.46(12)
O1–Ni1–O6^1	85.67(11)	N1–Ni2–O3	89.55(18)	O2–Ni2–O5	88.18(12)	O6–Ni2–O3	93.22(13)
O1^1–Ni1–O7	91.29(13)	N1–Ni2–O5	81.49(14)	O2–Ni2–O6	98.55(12)	O6–Ni2–O8	84.89(12)
O6–Ni1–O7	78.25(11)	N1–Ni2–O6	91.81(14)	O2–Ni2–O8	90.11(12)		

Symmetry transformations used to generate equivalent atoms: ^{1} $1-x$, $+y$, $1/2-z$.

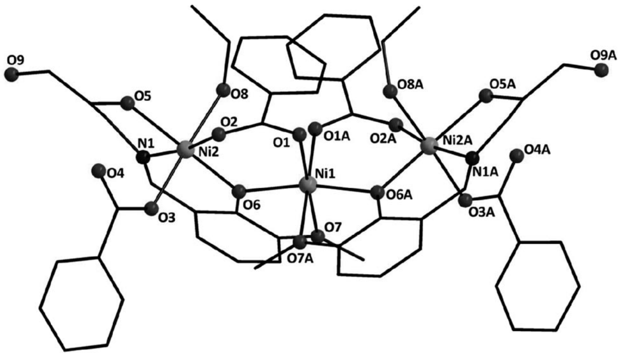

Figure 4. Coordination environment for complex **3**, the hydrogen atoms are omitted for clarity.

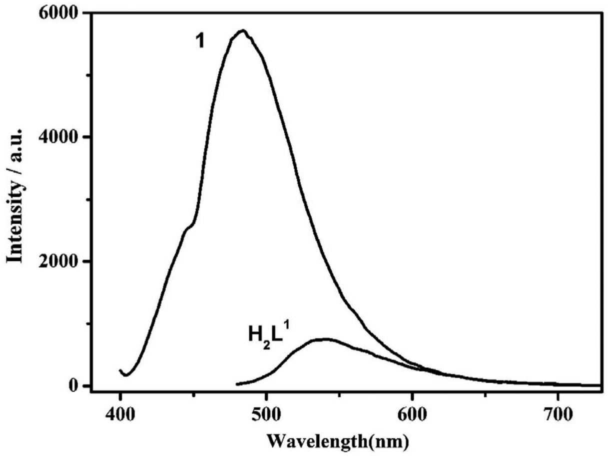

Figure 5. Normalized emission spectra of Schiff base ligand H_2L^1 and complex **1** in the solid state at room temperature.

Magnetic Properties

The magnetic properties of complexes **2** and **3** were studied to evaluate the magnetic interactions between the metallic ion centers. Variable temperature magnetic susceptibility measurements from 2 to 300 K under a constant magnetic field of 1 kOe were carried out. The $\chi_M T$ and χ_M vs. T plots are shown in Figure 6 and Figure 7 for compound **2** and **3**, respectively.

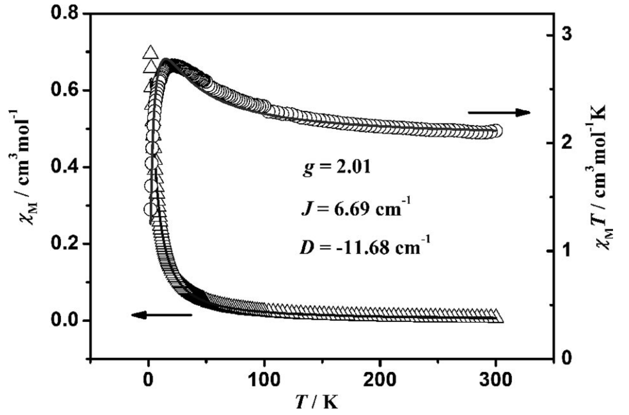

Figure 6. Plots of χ_M and $\chi_M T$ vs. T for complex **2**. The solid lines represent the best fits.

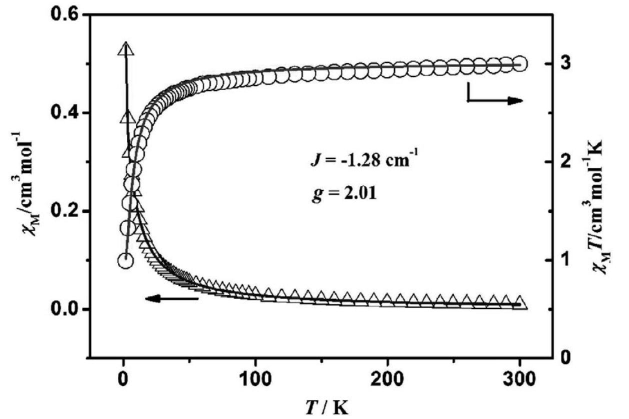

Figure 7. Plots of χ_M and $\chi_M T$ vs. T for complex **3**. The solid lines represent the best fits.

At room temperature, magnetic susceptibility data per $[Ni_2ON]$ entity for **2** shows a $\chi_M T$ value of 2.13 cm^3 mol^{-1} K (see Figure 6) which is very close to the spin only value of two Ni^{II} ions (2 cm^3 mol^{-1} K). Plots of $\chi_M T$ vs. T increase with decreasing temperature and reach a maximum at 20 K then follows by a rapidly decrease until 2 K. This behavior indicates a characteristic feature of intramolecular ferromagnetic interactions between metal centers of **2**. The sharp decrease of $\chi_M T$ value at very low temperature region may be attributed to zero-field splitting phenomenon. According to the structure of complex **2**, two central ions are bridged through nitrogen atom of EO azide group and phenolate oxygen atom from Schiff base ligand H_2L^1. According to the literature, the ferromagnetic interaction between Ni^{II} ions has been observed in μ_2-phenolate oxygen bridged[20] and EO azide bridged[21] binuclear nickel complexes. Actually, in the case of EO-azide bridging mode, the coupling between the bridged paramagnetic metal ions is ferromagnetic for a wide range of M–N–M angles.[22]

For the theoretical analysis of the magnetic behavior of compound **2**, the analytical expression based upon the Hamiltonian[23] was used.

$$\hat{H} = -2J\hat{S}_1\hat{S}_2 - D(\hat{S}_{1z}{}^2 + \hat{S}_{2z}{}^2) - g\beta H(\hat{S}_1 + \hat{S}_2)$$

Accordingly, the temperature dependence of the magnetic susceptibility of compound **2** was fitted, in which J is the usual intramolecular exchange parameter, D is the zero-field splitting term of the $^3A_2$ ground state. The best fit using the above equation was obtained with values of J = 6.69 cm^{-1}, D = –11.68 cm^{-1}, g = 2.01 and the agreement factor $R = \Sigma[(\chi_M)_{obs}-(\chi_M)_{calc}]^2/\Sigma\ [(\chi_M)_{obs}]^2 = 7.55\times 10^{-4}$. This result indicates that the complex **2** undergoes a ferromagnetic spin-exchange interaction between the metal ions. The coupling interactions in the binuclear magnetic entity are relatively strong, which is consistent with the reported binuclear Ni^{II} complex in literature.[24]

As shown in Figure 7, the χ_MT value of 2.98 $cm^3\ mol^{-1}$ K at room temperature for complex **3** is slightly lower than the spin-only (g = 2) value of 3 $cm^3\ mol^{-1}$ K expected for a Ni_3^{II} unit. As the temperature decreases, χ_MT decreases smoothly until 50 K, on further cooling the χ_MT value starts decreasing abruptly to 1.01 $cm^3\ mol^{-1}$ K at 2.0 K. This behavior indicates the typical antiferromagnetic interactions between the magnetic centers. According to the trinuclear nickel core structure of complex **3**, the coupling mode can be expressed as the spin Hamiltonian[25] $\hat{H} = -2J\ (\hat{S}_1\hat{S}_2 + \hat{S}_2\hat{S}_3)$. Thus, the temperature dependence of χ_M was modeled. Least-squares best-fit parameters are J = –1.28 cm^{-1}, g = 2.01 and $R = 2.34 \times 10^{-4}$ ($R = \Sigma[(\chi_M)_{obs}-(\chi_M)_{calc}]^2/\Sigma[(\chi_M)_{obs}]^2$). The above model provides a good fit over the temperature range 2–300 K. This result indicates that the complex **3** undergoes a weak antiferromagnetic spin-exchange interaction between the metal ions. The coupling interactions in the trinuclear magnetic entity are weak, which is consistent with the reported trinuclear Ni^{II} complex in former literature.[26]

Conclusions

One novel zinc(II) complex $[Zn_3(HL^1)_3(\mu_3\text{-}CH_3O)]\cdot(ClO_4)_2(H_2O)_3$ (**1**) and two new nickel(II) complexes $[Ni_2(HL^1)_2(\mu_{1,1}\text{-}N_3)(o\text{-vanillin})]\cdot H_2O$ (**2**), $[Ni_3(HL^2)_2(PhCOO)_2(PhCOOH)_2\cdot(EtOH)_2]$ (**3**) have been synthesized by using metal ions and potentially multidentate Schiff base ligands. Single crystal X-ray diffraction reveal that central metal ions in complexes **1**, **2** and **3** are all bridged by phenolate oxygen atom from Schiff base ligands. The solid state luminescent spectra demonstrates complex **1** displays much stronger emission intensity than that of Schiff base ligand H_2L^1 with a slightly blue-shift. The fitting magnetic results confirm that complex **2** exhibits ferromagnetic coupling whereas complex **3** exhibits antiferromagnetic coupling between the Ni^{II} ions. The next work to design and synthesize nickel and zinc complexes with various nuclear numbers which may exhibit interesting properties and applications is under investigation in our lab.

Experimental Section

General: *o*-Vanillin, 2-amino-2-methyl-1-propanol, 3-amino-1,2-propanediol were obtained from Aldrich. The other reagents were all laboratory originally. All the starting reagents were of A.R. grade and were used as purchased. Elemental analyses for carbon, hydrogen and nitrogen were carried out with a Perkin–Elmer 2400 Elemental Analyzer. Fourier transform infrared (FTIR) spectra were recorded with a Bruker Tensor 27 spectrophotometer using the reflectance technique (4000–400 cm^{-1}). Samples were prepared as KBr disks. The luminescence spectra for the powdered solid samples were measured at room temperature on a FLS920 fluorescence spectrophotometer. The excitation slit and the emission slit were 0.5 nm. Variable temperature magnetic susceptibility measurements were performed in the temperature range 2–300 K using a Quantum Design MPMS XL-7 SQUID magnetometer at a magnetic field of 1000 Oe. The diamagnetic corrections for the compounds were estimated using Pascal's constants, and magnetic data were corrected for diamagnetic contributions of the sample holder.

Synthesis of Schiff Base Ligands: The Schiff base ligand H_2L^1 was prepared as described elsewhere.[14] The Schiff base ligand H_3L^2 was synthesized by a reflux reaction between *o*-vanillin (760 mg, 5 mmol) and 3-amino-1,2-propanediol (455 mg, 5 mmol) in methanol (10 mL). The resulting orange yellow solution containing the required product was used without further purification. The concentration of both ligands solution is 0.5 mmol mL^{-1}.

$[Zn_3(HL^1)_3(\mu_3\text{-}CH_3O)]\cdot(ClO_4)_2(H_2O)_3$ (1): $Zn(ClO_4)_2\cdot 6H_2O$ (186 mg, 0.5 mmol) was added to a solution of H_2L^1 (1 mL, 0.5 mmol) in methanol/dichloromethane (24 mL, 1:2 v/v). The mixture was filtered after further stirring for 20 min and a light yellow solution was obtained. After several days standing at room temperature, yellow crystals suitable for X-ray diffraction analysis were collected. Yield: ca. 54 % based on $Zn(ClO_4)_2\cdot 6H_2O$. Elemental analysis: $C_{37}H_{51}Cl_2N_3O_{21}Zn_3$ (1140.82): C 54.54 (calcd. 54.01); H 4.68(calcd. 4.88), N 2.37(calcd. 2.36) %. **IR** (KBr, selected data): ν = 3421 (m), 3157 (m), 2972 (m), 2835 (w), 1629 (s), 1562 (w), 1467 (s), 1400 (s), 1305 (m), 1247 (s), 1107 (s), 968 (m), 858 (w), 736 (s), 624 (s), 567 (w), 470 (w) cm^{-1}.

$[Ni_2(HL^1)_2(\mu_{1,1}\text{-}N_3)(o\text{-vanillin})]\cdot H_2O$ (2): $Ni(ClO_4)_2\cdot 6H_2O$ (176 mg, 0.5 mmol) was dissolved in a solution of H_2L^1 (1 mL, 0.5 mmol) in methanol/dichloromethane (24 mL, 1:2 v/v). Afterwards, NaN_3 (65 mg, 1 mmol) in 1 mL aqueous solution was added dropwise with stirring. The mixture was filtered after further 20 min stirring, the resulting dark green solution was obtained. After several days standing at room temperature, diamond-shaped dark green crystals that suitable for X-ray diffraction analysis were collected. Yield: ca. 61 % based on $Ni(ClO_4)_2\cdot 6H_2O$. Elemental analysis: $C_{32}H_{41}N_5Ni_2O_{10}$ (773.12): C 49.21 (calcd. 49.59), H 5.14 (calcd. 5.59), N 9.54 (calcd. 9.04) %. **IR** (KBr, selected data): ν = 3427 (m), 3159 (m), 1633 (m), 1556 (m),

Table 5. Crystallographic data and structure refinements for complexes **1**–**3**.

	1	**2**	**3**
Empirical formula	$Zn_3C_{37}H_{57}Cl_2N_3O_{21}$	$Ni_2C_{32}H_{43}N_5O_{10}$	$Ni_3C_{54}H_{58}N_2O_{18}$
Formula weight	1146.92	776.12	1199
Temperature /K	293(2)	296(2)	293(2)
Crystal system	triclinic	triclinic	monoclinic
Space group	$P\bar{1}$	$P\bar{1}$	$C2/c$
a /Å	13.420(2)	10.1165(16)	21.551(4)
b /Å	13.617(2)	12.5769(19)	9.2719(19)
c /Å	17.866(2)	14.218(2)	29.551(6)
α /°	69.577(13)	74.4670(10)	90.00
β /°	82.469(12)	84.084(2)	103.47(3)
γ /°	60.492(16)	83.050(2)	90.00
Volume /Å^3	2659.4(7)	1725.4(5)	5742(2)
Z	2	2	4
ρ_{calc} /mg·mm^{-3}	1.430	1.488	1.387
μ /mm^{-1}	1.514	1.154	1.044
F(000)	1180.0	812.0	2496.0
Theta range/°	5.86 to 50.04°	4.86 to 50°	4.8 to 50.02°
Index ranges (h, k, l)	$-14 \leq h \leq 15$ $-15 \leq k \leq 16$ $-21 \leq l \leq 21$	$-12 \leq h \leq 11$ $-14 \leq k \leq 14$ $-16 \leq l \leq 16$	$-24 \leq h \leq 25$ $-11 \leq k \leq 11$ $-34 \leq l \leq 33$
Reflections collected	17215	11852	22229
Data/restraints/parameters	9348/260/715	5970/7/461	5007/1146/367
Goodness-of-fit on F^2	1.054	1.041	1.102
Final R indexes [$I \geq 2\sigma(I)$]	$R_1 = 0.0751$, $wR_2 = 0.2180$	$R_1 = 0.0374$, $wR_2 = 0.0929$	$R_1 = 0.0845$, $wR_2 = 0.1954$
Final R indexes [all data]	$R_1 = 0.0978$, $wR_2 = 0.2446$	$R_1 = 0.0520$, $wR_2 = 0.1037$	$R_1 = 0.0969$, $wR_2 = 0.2031$

a) $R = \Sigma||F_o|-|F_c||/\Sigma|F_o|$, b) $wR = [\Sigma[w(F_o^2 - F_c^2)^2]/\Sigma[(wF_0^2)^2]]^{1/2}$.

1465 (s), 1404 (s), 1303 (m), 1218 (s), 1105 (s), 972 (w), 860 (w), 738 (m), 626 (m), 470 (w) cm^{-1}.

$[Ni_3(HL^2)_2(PhCOO)_2(PhCOOH)_2(EtOH)_2]$ (3): $NiCl_2·6H_2O$ (238 mg, 1 mmol) was added to a solution of H_3L^2 (2 mL, 1 mmol) in ethanol (20 mL), afterwards Et_3N (200 mg, 2 mmol) and formic acid (92 mg, 2 mmol) were added to the mixture. The solution was stirred for 30 min, and afterwards sodium benzoate (144 mg, 1 mmol) was added with stirring. The resulting dark green solution was filtered after being stirred for another 30 minutes at room temperature. Upon slow evaporation of the solvents, dark green crystals formed from the filtrate in a few days. Yield: ca. 58% based on $NiCl_2·6H_2O$. Elemental analysis: $Ni_3C_{54}H_{58}N_2O_{18}$ (1199): C 53.98 (calcd. 54.09) H 4.90 (calcd. 4.87) N 2.45 (calcd. 2.34). **IR** (KBr, selected data): ν = 3787 (w), 3413 (s), 2942 (m), 2047 (w), 1658 (s), 1600 (s), 1550 (s), 1398 (s), 1288 (m), 1217 (s), 1078 (m), 848 (w), 724 (m), 681 (m) cm^{-1}.

Crystal Structure Determination: X-ray measurements for **1**, **2**, and **3** were taken at room temperature on a Bruker ApexII CCD diffractometer with graphite-monochromated Mo-K_α radiation (λ = 0.71073 Å), operating in ω–2θ scanning mode using suitable crystals for data collection. Lorentz-polarization correction was applied to the data. The structure was solved by direct methods and refined by full-matrix least-squares procedures on F^2 using SHELX-97.[27] Some hydrogen atoms of the solvent water molecules in complex **1** are not included in the model because the structure of the water molecular was refined by disorder treatment and some of the hydrogen atoms are hard to calculate their positions. All the other hydrogen atoms were added theoretically and refined with riding model position parameters and fixed isotropic thermal parameters. The bad R-values of complexes **1** and **3** may be caused by low crystal quality. Crystallographic data and refinement details for complexes **1**–**3** are given in Table 5. Crystallographic data (excluding structure factors) for the structures in this paper have been deposited with the Cambridge Crystallographic Data Centre, CCDC, 12 Union Road, Cambridge CB21EZ, UK. Copies of the data can be obtained free of charge on quoting the depository numbers CCDC-942647, CCDC-942648, and CCDC-942649 (Fax: +44-1223-336-033; E-Mail: deposit@ccdc.cam.ac.uk, http://www.ccdc.cam.ac.uk).

Acknowledgments

Financial support by the National Natural Science Foundation of China (21061009) and Inner Mongolia Autonomous Region Fund for Natural Science (2013ZD09) are kindly acknowledged.

References

[1] a) T. C. Stamatatos, A. G. Christou, S. Mukherjee, K. M. Poole, C. Lampropoulos, K. A. Abboud, T. A. O'Brien, G. Christou, *Inorg. Chem.* **2008**, *47*, 9021–9034; b) C. Lampropoulos, K. A. Abboud, T. C. Stamatatos, G. Christou, *Inorg. Chem.* **2009**, *48*, 813–815.

[2] T. Kajiwara, M. Nakano, Y. Kaneko, S. Takaishi, T. Ito, M. Yamashita, A. Igashira-Kamiyama, H. Nojiri, Y. Ono, N. Kojima, *J. Am. Chem. Soc.* **2005**, *127*, 10150–10151.

[3] J. Xu, X. Sun, Y. Fan, C. Bi, M. Sun, *Z. Anorg. Allg. Chem.* **2012**, *638*, 1512–1518.

[4] a) C. K. Brozek, M. Dincă, *Chem. Sci.* **2012**, *3*, 2110; b) D. L. Reger, J. J. Horger, M. D. Smith, G. J. Long, F. Grandjean, *Inorg. Chem.* **2011**, *50*, 686–704; c) H. Li, M. Eddaoudi, T. L. Groy, O. M. Yaghi, *J. Am. Chem. Soc.* **1998**, *120*, 8571–8572.

[5] a) T. C. Stamatatos, D. Foguet-Albiol, C. C. Stoumpos, C. P. Raptopoulou, A. Terzis, W. Wernsdorfer, S. P. Perlepes, G. Christou, *J. Am. Chem. Soc.* **2005**, *127*, 15380–15381; b) T. C. Stamatatos, D. Foguet-Albiol, S.-C. Lee, C. C. Stoumpos, C. P. Raptopoulou, A. Terzis, W. Wernsdorfer, S. O. Hill, S. P. Perlepes, G. Christou, *J. Am. Chem. Soc.* **2007**, *129*, 9484–9499; c) T. C. Stamatatos, K. A. Abboud, W. Wernsdorfer, G. Christou, *Polyhedron* **2007**, *26*, 2095–2100.

[6] a) X.-H. Lu, Y.-Q. Huang, L.-Y. Kong, T.-a. Okamura, W.-Y. Sun, N. Ueyama, *Z. Anorg. Allg. Chem.* **2007**, *633*, 2064–2070; b) L. Zhang, Y. Ji, X. Xu, Z. Liu, J. Tang, *J. Lumin.* **2012**, *132*, 1906–1909.

[7] H.-X. Li, W. Zhao, H.-Y. Li, Z.-L. Xu, W.-X. Wang, J.-P. Lang, *Chem. Commun.* **2013**, *49*, 4259.

[8] J. D. Henthorn, N. Mishra, C. D. Haun, A. L. Castro, H. G. Douglas, M. Pegram, B. Stadelmaier, J. S. Huebner, C. Lampropoulos, *Polyhedron* **2013**, *53*, 62–66.

[9] S.-M. Ying, *Inorg. Chem. Commun.* **2012**, *22*, 82–84.

[10] J. Cao, Y. Gao, Y. Wang, C. Du, Z. Liu, *Chem. Commun.* **2013**, *49*, 6897.

[11] J. Xie, S. Cao, D. Good, M. Wei, X. Ren, *Inorg. Chem.* **2010**, *49*, 1319–1321.

[12] N. Kielland, E. C. Escudero-Adán, M. Martínez Belmonte, A. W. Kleij, *Dalton Trans.* **2013**, *42*, 1427.

[13] a) R. Biswas, S. Mukherjee, P. Kar, A. Ghosh, *Inorg. Chem.* **2012**, *51*, 8150–8160; b) R. Biswas, S. Giri, S. K. Saha, A. Ghosh, *Eur. J. Inorg. Chem.* **2012**, 2916–2927.

[14] Y.-F. Ji, R. Wang, S. Ding, C.-F. Du, Z.-L. Liu, *Inorg. Chem. Commun.* **2012**, *16*, 47–50.

[15] a) M.-L. Tong, S.-L. Zheng, J.-X. Shi, Y.-X. Tong, H. K. Lee, X.-M. Chen, *J. Chem. Soc., Dalton Trans.* **2002**, 1727–1734; b) B. Sarkar, M. S. Ray, Y.-Z. Li, Y. Song, A. Figuerola, E. Ruiz, J. Cirera, J. Cano, A. Ghosh, *Chem. Eur. J.* **2007**, *13*, 9297–9309.

[16] A. K. Ghosh, A. Bauzá, V. Bertolasi, A. Frontera, D. Ray, *Polyhedron* **2013**, *53*, 32–39.

[17] W.-K. Dong, Y.-X. Sun, G.-H. Liu, L. Li, X.-Y. Dong, X.-H. Gao, *Z. Anorg. Allg. Chem.* **2012**, *638*, 1370–1377.

[18] D. Das, B. G. Chand, K. K. Sarker, J. Dinda, C. Sinha, *Polyhedron* **2006**, *25*, 2333–2340.

[19] a) Q. Shi, L. Sheng, K. Ma, Y. Sun, X. Cai, R. Liu, S. Wang, *Inorg. Chem. Commun.* **2009**, *12*, 255–258; b) H.-H. Li, Z.-L. You, C.-L. Zhang, M. Yang, L.-N. Gao, L. Wang, *Inorg. Chem. Commun.* **2013**, *29*, 118–122; c) G.-X. Liu, Y.-Y. Xu, Y. Wang, S. Nishihara, X.-M. Ren, *Inorg. Chim. Acta* **2010**, *363*, 3932–3938.

[20] Y. Zhang, X.-M. Zhang, T.-F. Liu, W.-G. Xu, *Transit. Met. Chem.* **2010**, *35*, 851–858.

[21] G. Manca, J. Cano, E. Ruiz, *Inorg. Chem.* **2009**, *48*, 3139–3144.

[22] a) S. K. Dey, N. Mondal, M. S. El Fallah, R. Vicente, A. Escuer, X. Solans, M. Font-Bardía, T. Matsushita, V. Gramlich, S. Mitra, *Inorg. Chem.* **2004**, *43*, 2427–2434; b) E. Ruiz, J. Cano, S. Alvarez, P. Alemany, *J. Am. Chem. Soc.* **1998**, *120*, 11122–11129.

[23] S. Liang, Z. Liu, N. Liu, C. Liu, X. Di, J. Zhang, *J. Coord. Chem.* **2010**, *63*, 3441–3452.

[24] S.-Y. Zhang, B. Xu, L. Zheng, W. Chen, Y. Li, W. Li, *Inorg. Chim. Acta* **2011**, *367*, 44–50.

[25] X.-H. Bu, M. Du, L. Zhang, D.-Z. Liao, J.-K. Tang, R.-H. Zhang, M. Shionoya, *J. Chem. Soc., Dalton Trans.* **2001**, 593–598.

[26] Y.-Z. Tong, Q.-L. Wang, M. Si, J. Qi, S.-P. Yan, G.-M. Yang, P. Cheng, D.-Z. Liao, *Polyhedron* **2011**, *30*, 3151–3157.

[27] G. M. Sheldrick, *SHELXS-97: Programs for X-ray Crystal Structure Solution*, University of Gottingen: Germany, **1997**.

Received: June 8, 2013